Long-term observations of the background aerosol at Cabauw, The Netherlands

Mamali, D.; Mikkilä, J.; Henzing, B; Spoor, R.; Ehn, M.; Petäjä, T.; Russchenberg, H.; Biskos, G.

DOI
10.1016/j.scitotenv.2017.12.136

Publication date
2018

Document Version
Final published version

Published in
Science of the Total Environment

Science of the Total Environment 625 (2018) 752–761

Contents lists available at ScienceDirect

Science of the Total Environment

journal homepage: www.elsevier.com/locate/scitotenv

Long-term observations of the background aerosol at Cabauw, The Netherlands

D. Mamali[a,*], J. Mikkilä[b], B. Henzing[c], R. Spoor[d], M. Ehn[b], T. Petäjä[b], H. Russchenberg[a], G. Biskos[a,e,**]

[a] Faculty of Civil Engineering and Geosciences, Delft University of Technology, Delft 2628 CN, The Netherlands
[b] Department of Physics, University of Helsinki, P.O. Box 64, Helsinki 00014, Finland
[c] Netherlands Organisation for Applied Scientific Research TNO, Princetonlaan 6, Utrecht 3508 TA, The Netherlands
[d] National Institute of Public Health and the Environment RIVM, Bilthoven 3720 BA, The Netherlands
[e] Energy Environment and Water Research Center, The Cyprus Institute, Nicosia 2121, Cyprus

HIGHLIGHTS

- We report 8-year-long measurements of that atmospheric aerosol observed at Cabauw.
- $PM_{2.5}$ exhibit an overall decrease with a trend of −0.74 μm m^{-3} $year^{-1}$.
- Particle number concentrations are stable with a mean value of 9.2 × 10^3 # cm^{-3}.
- Highest particle concentrations are observed in winter and spring.
- Particle hygroscopicity shows that the aerosol is often externally mixed.

GRAPHICAL ABSTRACT

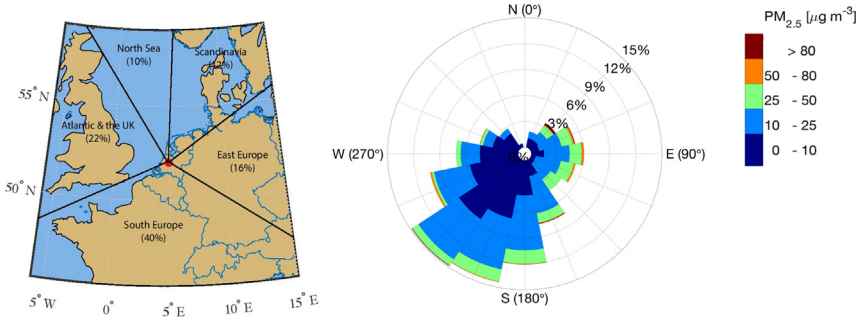

ARTICLE INFO

Article history:
Received 20 September 2017
Received in revised form 10 November 2017
Accepted 12 December 2017
Available online 4 January 2018

Editor: Xuexi Tie

Keywords:
Air pollution
Atmospheric particles
$PM_{2.5}$
SMPS
HTDMA

ABSTRACT

Long-term measurements of $PM_{2.5}$ mass concentrations and aerosol particle size distributions from 2008 to 2015, as well as hygroscopicity measurements conducted over one year (2008–2009) at Cabauw, The Netherlands, are compiled here in order to provide a comprehensive dataset for understanding the trends and annual variabilities of the atmospheric aerosol in the region. $PM_{2.5}$ concentrations have a mean value of 14.4 μg m^{-3} with standard deviation 2.1 μg m^{-3}, and exhibit an overall decreasing trend of −0.74 μg m^{-3} $year^{-1}$. The highest values are observed in winter and spring and are associated with a shallower boundary layer and lower precipitation, respectively, compared to the rest of the seasons. Number concentrations of particles smaller than 500 nm have a mean of 9.2 × 10^3 particles cm^{-3} and standard deviation 4.9 × 10^3 particles cm^{-3}, exhibiting an increasing trend between 2008 and 2011 and a decreasing trend from 2013 to 2015. The particle number concentrations exhibit highest values in spring and summer (despite the increased precipitation) due to the high occurrence of nucleation-mode particles, which most likely are formed elsewhere and are transported to the observation station. Particle hygroscopicity measurements show that, independently of the air mass origin, the particles are mostly externally mixed with the more hydrophobic mode having a mean hygroscopic parameter κ of 0.1 while for the more hydrophilic mode κ is 0.35. The hygroscopicity of the smaller particles investigated in this work (i.e., particles having diameters of 35 nm) appears to increase during the course of the nucleation events, reflecting a change in the chemical composition of the particles.

* Corresponding author.
** Correspondence to: G. Biskos, Energy Environment and Water Research Centre, The Cyprus Institute, Nicosia 2121, Cyprus & Faculty of Civil Engineering and Geosciences, Delft University of Technology, Delft 2628 CN, The Netherlands.
E-mail addresses: D.Mamali@tudelft.nl (D. Mamali), G.Biskos@cyi.ac.cy, G.Biskos@tudelft.nl (G. Biskos).

https://doi.org/10.1016/j.scitotenv.2017.12.136
0048-9697/

1. Introduction

Epidemiological and medical studies have established that Particulate Matter (PM) pollution has a strong impact on human health (e.g., US-EPA, 2004; Pope and Dockery, 2006; Baccarelli et al., 2016), with elevated ambient $PM_{2.5}$ concentrations being associated with adverse respiratory effects to chronically ill patients and increased mortality rates for people with respiratory problems (Wichmann and Peters, 2000). In addition, fine particles (i.e., particles with diameters below 1 μm), and especially their smallest fraction that can penetrate deeper in the respiratory tract and reach the alveoli (Asgharian et al., 2014), can enter the blood recirculation system and cause cardiovascular deceases (Zlotkowska, 2015). Model studies have shown that $PM_{2.5}$ concentrations correlate well with morbidity and mortality, causing ca. 3.3 million premature deaths annually around the globe (e.g., Lelieveld et al., 2015).

Apart from being related to adverse health effects, airborne particles emitted from natural and anthropogenic sources can affect the climate of our planet at local, regional and global scales. Air-suspended particles affect climate in a direct way by absorbing and scattering incoming solar radiation (Ramanathan et al., 2001), and indirectly by acting as cloud condensation and ice nuclei (CCN and IN, respectively; Lohmann and Feichter, 2005). Both effects result in an overall cooling of the Earth and together can contribute to a forcing of -1 W/m^2 at the top of the atmosphere with an estimated uncertainty of the order of 100% (Solomon, 2007). This high uncertainty results from the high spatial and temporal variability of the atmospheric aerosol as well as from the poor understanding of key physicochemical transformations that the aerosol particles undergo during their lifetime. To better understand their role on climate, and thus to improve the predictability of atmospheric-climate models, we need long-term measurements of the aerosol properties. Apart from the concentration (by mass and number) of airborne particles, information on the temporal variability of their size and chemical composition is highly required for understanding the processes they are involved in.

The Cabauw Experimental Site for Atmospheric Research (CESAR) in The Netherlands is one of the oldest stations for atmospheric observations in Europe, and one of the core observatories in the global network. CESAR is one of the few observatories where characterization of the atmosphere from the ground up to the top of the atmospheric column is taking place by combining in situ sensors installed at the ground level and at different heights on a 213-m tower, as well as ground-based remote sensing instruments for measuring radiation, wind, turbulence, trace gases, aerosols, and clouds at higher altitudes. Continuous long-term in-situ measurements of the mass concentrations and the number size distributions of atmospheric particles are performed at CESAR since more than a decade. In addition, measurements related to the atmospheric state and various atmosphere-land surface interactions for supporting climate modeling are carried out at CESAR using both in-situ and remote sensing techniques (Russchenberg et al., 2005).

Here we report $PM_{2.5}$ mass concentration and aerosol size distribution measurements conducted at Cabauw from 2008 to 2015, and analyze their trends and seasonal variability. In addition, we provide aerosol hygroscopicity measurements that took place over almost one year (10 months), and link them with the patterns observed in the recorded size distributions. The rest of the paper is organized as follows: Section 2 describes the instrumentation used for the measurements. Section 3 discusses the measurements, including the inter-annual and seasonal variations of $PM_{2.5}$ concentrations and the particle number distributions, as well as the seasonality in particle hygroscopicity. Finally Section 4 summarizes the most important conclusions.

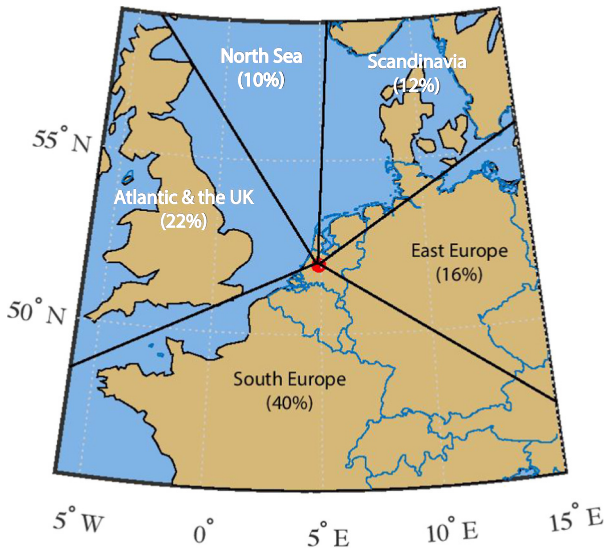

Fig. 1. Location of the CESAR and annual relative frequency of the wind directions observed at the site during the study period.

2. Instrumentation and methods

2.1. The Cabauw Experimental Site for Atmospheric Research (CESAR)

CESAR is a rural site in a region that is one of the most populated areas in Europe (Gallego, 2010). The station, located 50 km away from the coast, is surrounded by grassland and agricultural pastures, and is influenced by maritime and continental environments. The terrain in the region is flat, varying from −3 to 5 m a.s.l. within a radius of 45 km. Fig. 1 shows the location of the station and the frequency of the different wind directions based on measurements recorded between 2008 and 2015 at the tower of the station (cf. Fig. S1 that shows the wind rose diagrams of each year for more details). The site most often receives continental air masses from Southern Europe (40%), with the predominant wind directions being Southwestern (SW), advecting polluted air masses that pass over the neighboring city of Rotterdam. Clean air masses are associated with Northern (N) air originating from the North Sea or Scandinavia only if they do not follow trajectories over Amsterdam and Utrecht; i.e., the other two major neighboring cities to CESAR. Considering that the site mostly receives air masses passing over close-by cities and a dense highway grid located within a radius of 45 km, the station is representative of the wider region.

2.2. Instrumentation

A low-volume sampler operated at a flow rate of 2.3 m^3 h^{-1} and equipped with a $PM_{2.5}$ sampling head (complying with the EN 12341 standards) was deployed to measure the mass concentration of particles smaller than 2.5 μm on quartz filters (Whatman QM-A). All $PM_{2.5}$ measurements were performed by the Dutch National Institute of Public Health and the Environment (RIVM) at the Cabauw Wielsekade station (500 m away from the tower) where air was sampled at a height of 4 m a.s.l. The samples were collected every 24 h, and the mass of the particles deposited on the filters was determined gravimetrically (e.g., Triantafyllou et al., 2016). All the filters were conditioned at 20 ± 1°C and 50 ± 5% RH for at least 48 h before weighing (CEN, 2005). $PM_{2.5}$ measurements were performed on a daily basis during 2009 and 2015, while for the rest of the years investigated in this work, data were available every second day. During days without $PM_{2.5}$ measurements, the quartz filters

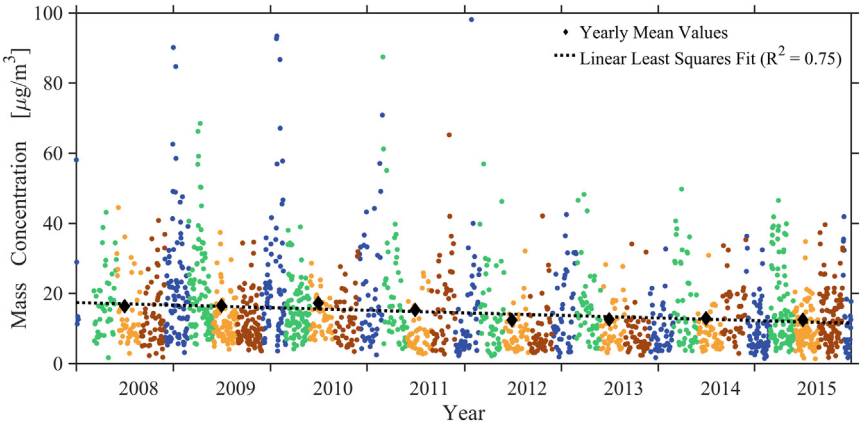

Fig. 2. $PM_{2.5}$ daily concentrations measured at Cabauw from January 2008 to December 2015. Daily measurements are represented by dots color-coded based based on the different seasons: blue for winter including the months from December to February, green for spring including the months from March to May, yellow for summer including the months from June to August and brown for autumn including the months from September, to November. The black line shows the $PM_{2.5}$ trend calculated based on the yearly mean values (black diamonds).

were replaced by Teflon or Tissuquartz filters used for Elemental or Organic Carbon analysis, respectively.

A Scanning Mobility Particle Sizer (SMPS; TSI Model 3034) was used to measure the size distributions of the particles having diameters in the range 9.37–516 nm. The SMPS consisted of an impactor, a charger, a Differential Mobility Analyzer (DMA) and a Condensation Particle Counter (CPC). Inversion of the collected data was performed with the algorithm described by Wiedensohler et al. (2012). Although the SMPS data used for this analysis cover the period from 2008 to 2015, the data from January to December 2012 were discarded due to high noise levels.

A Hygroscopic Tandem DMA (HTDMA) system was deployed in the framework of the EUCAARI IMPACT campaign to determine the hygroscopicity of the particles observed from May 2008 to February 2009 at CESAR. In brief, the system consists of two DMAs (cf. Winklmayr et al., 1991, for details) and a CPC (TSI Model 3772; Stolzenburg and McMurry, 1991). To reduce the humidity below 20% and comply with the EUSAAR standards (Duplissy et al., 2009), a custom-made Nafion drying system was used upstream the HTDMA, in addition to the sample drying system of the station. In the HTDMA, the polydisperse aerosol sample was first charge neutralized (by passing through a ^{85}Kr-source aerosol neutralizer) and then passed through the first DMA that selected particles of specific dry sizes (35, 50, 75, 110 and 165 nm) before being exposed at a constant RH of 90% in the humidifier of the system. The size distribution of the humidified particles was measured by the second DMA and a CPC. Both DMAs used sheath flows in closed loops (Jokinen and Mäkelä, 1997), whereas the measurement time for each particle size was 5 min. Values of the hygroscopic parameter κ, which are discussed in the following section, were determined by the HTDMA measurements (see, e.g., Bougiatioti et al., 2016a, b).

Both the SMPS and the HTDMA sampled air at 60 m a.s.l. through a specially-designed inlet system that consisted of four parts: (a) 4 PM_{10} inlets, (b) a Nafion-tube system that dried the aerosol stream to relative humidity values (RH) below 40%, (c) a 60-m stainless steel pipe and (d) a manifold that split the flow to the instrument suite (Zieger et al., 2011). The total flow through the 60-m long inlet pipe was maintained at about 60 l min^{-1}, which was the highest flow warranting laminar flow ($Re \approx 2000$) From this flow the SMPS and the HTDMA were sampling at a flow rate of 1 l min^{-1} each. For the SMPS data, corrections were applied to account for the diffusional losses of the particles on the walls of the 60-m sampling line (Henzing, 2011).

Meteorological measurements of wind direction, wind speed, temperature and relative humidity (cf. Table S1) at 40 m altitude were used in the analysis. In addition, back-trajectories of the air masses arriving at the station were calculated by the NOAA HYSPLIT model (Draxler and Hess, 1998; Draxler and Rolph, 2003).

3. Results and discussion

3.1. Particle mass and number concentrations

3.1.1. $PM_{2.5}$ intra-annual variation

Fig. 2 shows $PM_{2.5}$ daily concentrations measured at Cabauw from January 2008 to December 2015. The measurements exhibit an overall decreasing trend with a slope of −0.74 μg m^{-3} year^{-1}, calculated based on the yearly mean values. This trend is partly (28%) due to the absence of extreme mass concentrations of $PM_{2.5}$ > 50 μg m^{-3} from 2011 onwards, which are more frequent under Eastern winds (cf. Fig. 3; left figure). Analysis excluding these extreme values still showed a negative trend with a slope of −0.54 μg m^{-3} year^{-1}, suggesting that the overall decrease is mainly attributed to the reduction of the background aerosol concentration. Despite the decreasing trend, all the yearly averages (cf. Table S2) exceed the annual $PM_{2.5}$ limit of 10 μg m^{-3} of the World Health Organization (WHO).

Apart from the annual mean values, also the number of days with $PM_{2.5}$ concentrations higher than the WHO daily limit of 25 μg m^{-3} decreased substantially over the study period, especially in winter (data not shown). The majority of the limit exceedances are associated with stable atmospheric conditions (i.e. Convective Available Potential Energy, CAPE < 0; Seinfeld and Pandis, 2016), which aid the built-up of pollution. As shown in Fig. 3 (see right figure) those days are mostly associated with winds from the East (E; ca. 65% of the cases), advecting air masses that pass over the heavily industrialized Ruhr area in Germany, and from the South (S, ranging from SE to SW; ca. 20% of the cases), traveling over France and Belgium before reaching Cabauw. Only in few occasions (ca. 15% of the cases) the air masses had marine origin traveling from the SW over the Rotterdam and Antwerp harbor areas.

The overall decreasing trends of $PM_{2.5}$ (both in terms of annual mean concentrations and number of daily limit exceedance days) can be attributed to the more stringent European regulations for industrial emissions (Directive, 2008) and by the more advanced

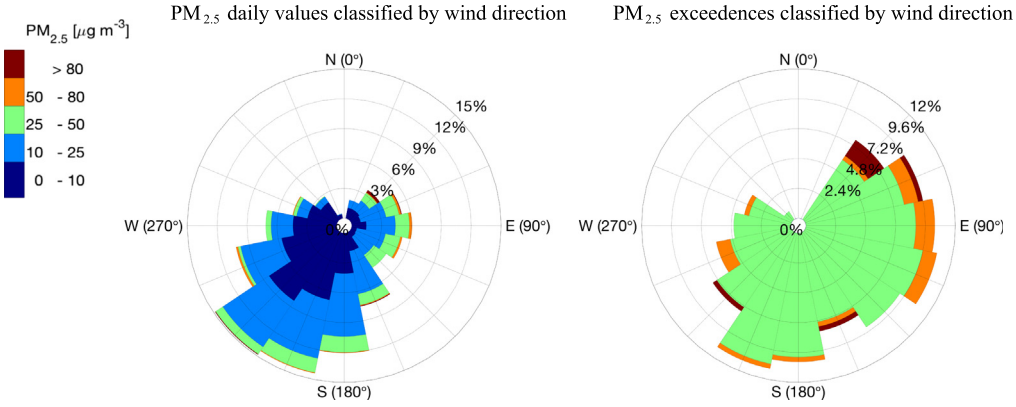

Fig. 3. $PM_{2.5}$ values (left) and $PM_{2.5}$ limit exceedances (right) segregated based on wind direction.

emission treatment technologies introduced in the transportation sector (it should be noted here that industry and transportation are two of the main contributors of $PM_{2.5}$ in The Netherlands and its neighboring countries; Matthijsen et al., 2007; EMEP). This hypothesis can be further supported by the similar decreasing pattern observed in the carbon monoxide (CO) measurements (cf. Fig. 4) which is mainly emitted from biomass burning, combustion and a number of industrial activities. The inter-annual variability of atmospheric factors influencing particle concentration (e.g., rain height, temperature, incoming solar radiation, as well as frequency and persistence of cold days with temperatures $<3\,^{\circ}C$) showed no statistically significant trends, suggesting that the reduced emissions are the main driver of the decreasing trend of $PM_{2.5}$.

3.1.2. $PM_{2.5}$ seasonal variation

The highest $PM_{2.5}$ concentrations throughout the study period were observed in winters and springs, with average values of 19.0 and 15.0 μg m^{-3}, respectively, whereas the lowest concentrations were observed in summers and autumns, having respective mean values of 9.1 and 10.8 μg m^{-3}. In general, high emissions from combustion sources (i.e., transportation and residential heating) in winter and autumn, and from agricultural activities in spring and summer, are the main contributors to this seasonal variation (Manders-Groot et al., 2016).

Apart from the local sources, $PM_{2.5}$ seasonal variability is also affected by the regional meteorological conditions including the variations in the wind speed that influences horizontal transport, in Boundary Layer Height (BLH) which is related to the dilution of the pollutants, and in precipitation that is the most important sink of PM pollution. Interestingly, only weak anti-correlation between wind speed and $PM_{2.5}$ concentrations (linear Pearson and non-linear Kendall correlation coefficient had respective values of $R_{Pearson} = -0.32$ and $\tau_{Kendall} = -0.27$; Gilbert, 1987; cf. Fig. S2) was observed despite the high wind speeds occurring in The Netherlands, suggesting that vertical dispersion (rather than natural ventilation) is the main process of dilution. Our analysis showed that the seasonal variability of the BLH influences the $PM_{2.5}$ concentrations (cf. Supplement for details) which is in line with previous studies (Pal et al., 2012, 2014). However, the low BLHs observed during winter cannot alone justify the higher $PM_{2.5}$ concentrations (cf. Fig. S3), and thus additional factors certainly contribute towards their seasonality. The rainfall height showed an anti-correlation with $PM_{2.5}$ ($R_{Pearson} = -0.68$, $\tau_{Kendall} = -0.51$, based on monthly average values) with the highest $PM_{2.5}$ concentrations observed in April, which is the driest month of the year (cf. Fig. 5a-b).

3.1.3. Particle number concentrations

Fig. 6 shows the number concentration of particles having diameters between 30 and 500 nm ($N_{30\text{-}500}$) measured at Cabauw from January 2008 to December 2015 (the measurements during 2012 were discarded due to high noise level). The mean number concentration of all years was 9.2×10^3 particles cm^{-3} with a standard deviation of 4.9×10^3 particles cm^{-3}. In contrast to the monotonic decrease of the $PM_{2.5}$ values, the particle number concentrations show an increasing trend of 8.1% $year^{-1}$ from 2008 to 2011 (calculated from the yearly mean values) and a decreasing trend of −11.7% $year^{-1}$ between 2013 and 2015. The predominant driver for these trends should be the aerosol sources since no corresponding changes were observed in the meteorological conditions in this period. More specifically, in terms of rainfall, which is the major aerosol sink, no

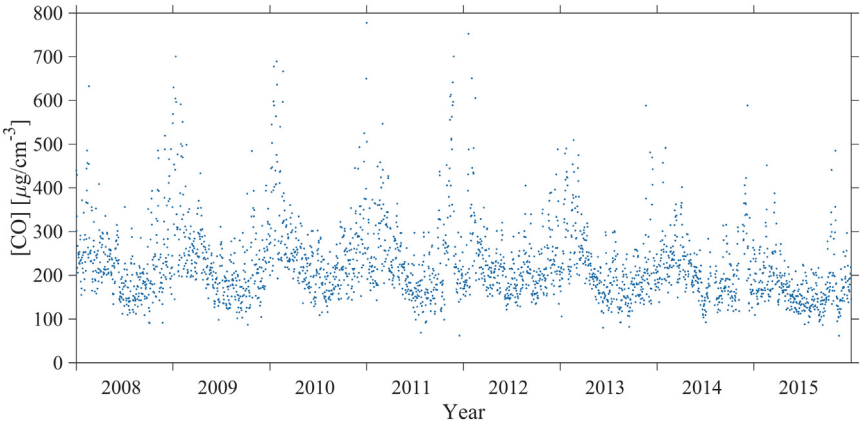

Fig. 4. Daily average CO concentrations measured at Cabauw from January 2008 to December 2015.

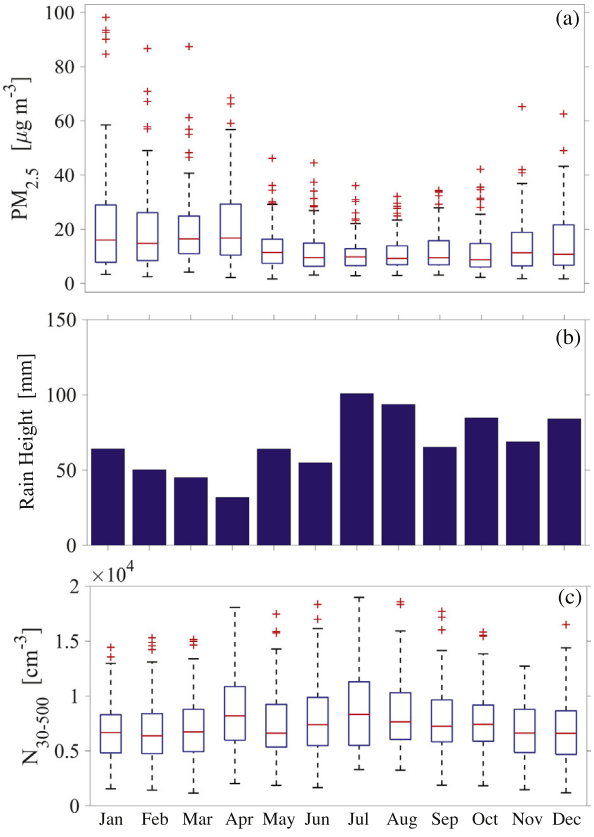

Fig. 5. (a) Monthly average $PM_{2.5}$ concentrations, (b) rainfall height, and (c) $N_{30\text{-}500}$ measured at CESAR from 2008 to 2015; The box plots in (a) and (c) indicate the median (red line) and the 25 and 75% percentile, whereas the red crosses are teh maximum values observed every month.

significant drop was recorded in years 2011 and 2013 when the highest $N_{30\text{-}500}$ values were measured. $PM_{0.5}$ mass concentrations estimated by the number concentration measurements assuming a constant particle density of 1.5 g cm^{-3} (data not shown) exhibit the same trend with the $N_{30\text{-}500}$, suggesting that the decreasing trend of the $PM_{2.5}$ is driven by a decrease of particles with diameters larger than 0.5 μm.

Seasonally, $N_{30\text{-}500}$ exhibits a strong anti-correlation with rainfall from January to June ($R_{Pearson} = -0.78$; Fig. 5), but in July and August, when the rain height reaches its maximum, the number of particles does not decrease, indicating that aerosol sources are also more and/or stronger during this period. The additional sources of particles in the warm period are possibly the new particle formation (NPF) events (see Section 3.2.2).

3.2. Aerosol particle size distributions

3.2.1. Diurnal and seasonal variation

Fig. 7 shows the diurnal variation of the mean particle number size distributions in the different seasons. The count median diameter (CMD) and geometric standard deviation of the background aerosol averaged over the entire study period are ca. 55 nm and 1.81, respectively. The diurnal variabilities in winter and autumn are very similar, with pronounced peaks observed during the late morning and evening hours corresponding to the traffic and residential heating peaks. Interestingly, in spring and summer, the distributions shift to smaller sizes after 12:00 UTC as a result of the frequent NPF events occurring during these periods. Comparison between weekends and weekdays (cf. Fig. S4) shows that the number concentration decreases by ca. 15% during the weekends for all seasons. In winter and autumn the peaks of the size distributions are less pronounced during the weekends as a result of the lower traffic density. Weekends during spring and summer exhibit intensified midday peaks due to more frequent NPF events (see discussion further below), which can be explained by the lower condensational sink as depicted in Fig. 8 (cf. similar observation in the measurements reported by Siakavaras et al., 2016). In an intra-annual basis, the annual mean CMD fluctuated slightly (within less than 10%), while the shape of the size distributions showed no significant changes (cf. Fig. S5).

3.2.2. New particle formation events

The particle number size distribution measurements show that numerous NPF events took place during the study period. To discriminate between an “event-day” and a “non-event” day, we used the procedure described in Dal Maso et al. (2005). In brief, we first examined the data visually, based on the 24-h (midnight to midnight) contour plots of the size distributions. A day was characterized as an event-day if the size distribution exhibited a new mode corresponding to particles smaller than 25 nm, followed by growth which lasted for several hours; otherwise it was labeled as a “non-event” day. This classification showed that NPF events occur at

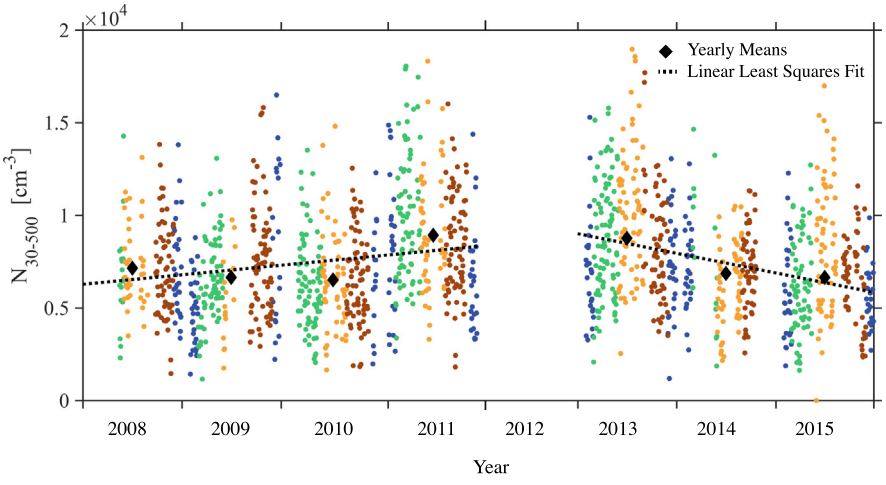

Fig. 6. $N_{30\text{-}500}$ concentrations measured at Cabauw from January 2008 to December 2015. Daily measurements are represented by dots color-coded based on the different seasons (blue for winter, green for spring, yellow for summer, and brown for autumn). The black dotted line shows the $N_{30\text{-}500}$ trend calculated based on the yearly mean values (black diamonds).

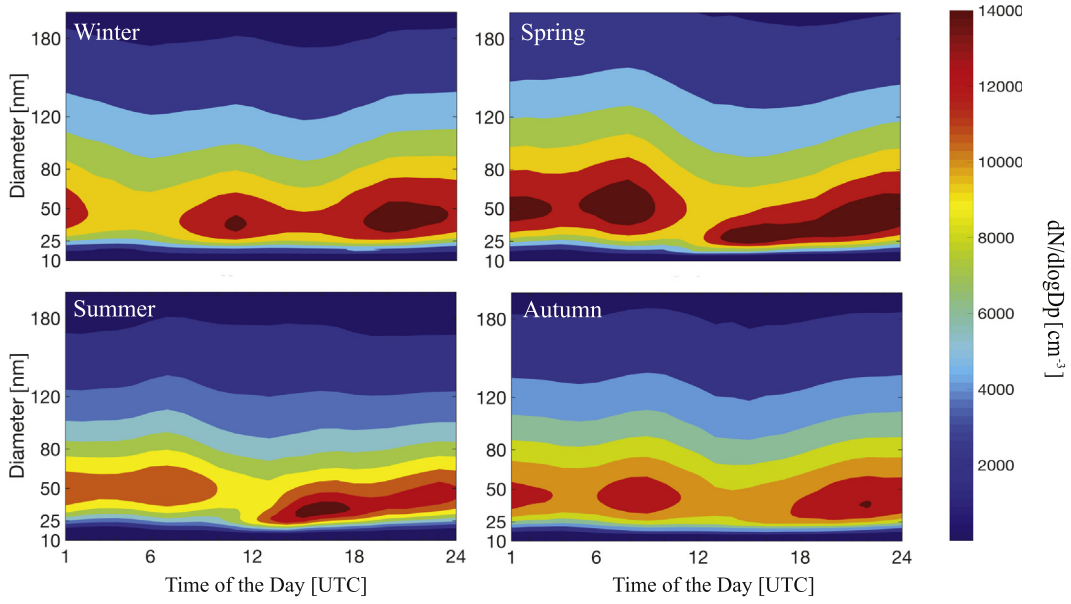

Fig. 7. Diurnal variation of the mean number size distributions during the different seasons.

Cabauw throughout the year but they are pronounced during spring and summer as has been observed in climatological studies at different locations in Europe (Birmili et al., 2001; Boulon et al., 2010). Our analysis focused on measurements from January 2010 to December 2011, when measurements down to 9.6 nm were available. Table 1 summarizes the number of NPFs for each month. The fraction of the number of "event-days" to the total number of (measurement) days was 20% in 2010 and 24% in 2011. All the events took place during daytime between 08:00 and 14:00 UTC, with the majority being observed under cloud free conditions. These observations are in line with those reported by Manninen et al. (2010), who investigated nucleation events and the first steps of growth, at many observatories in Europe, including Cabauw, using ion spectrometer measurements. Back-trajectory analysis (cf. Fig. S6) showed that NPF events are mostly related to marine air masses from the NW, N, W and SW (80%). These clean air masses having low particle number concentrations, and thus low condensational sinks, most often pass over cities (e.g. Amsterdam, Rotterdam) where they get enriched with gaseous pollutants which act as precursors for NPF. The rest of the events (20%) were recorded when air from the E and SE, that carry polluted air from Central Europe, reached Cabauw.

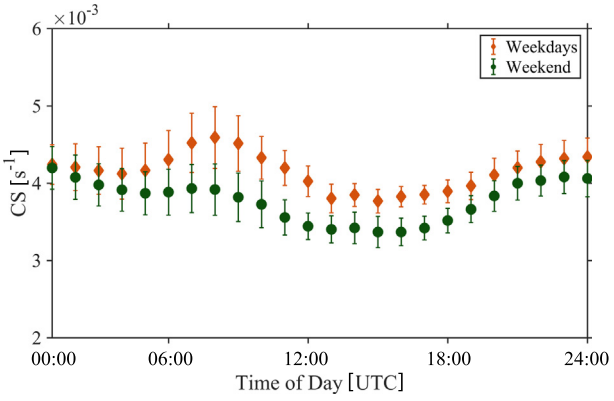

Fig. 8. Diurnal variation of the condensational sink during weekdays and weekends (error bars correspond to 1 standard deviation).

Characteristic NPF events, associated with air masses from the North Sea, are shown in Fig. 9. Solar radiation in the morning triggers the photochemical formation of new particles, which grow to detectable sizes within ~3–4 h. A steep increase in the number concentration of the smaller particles (having diameters up to 25 nm) was observed around 08:00–10:00 UTC. The small, newly formed particles slowly increase in size reaching that of the background aerosol late at night.

It should be noted here that the smallest particles for which increased concentrations were observed during the events had diameters of ca. 11 nm (note that the SMPS can measure from 9.6 nm and above), suggesting that the fresh particles were formed elsewhere and were advected to the site. This, however, is valid provided that the sub-11-nm channels of the SMPS do not underestimate the corresponding particle number concentrations significantly, and that the particles grow slow enough so that the time resolution of the instrument allows for capturing their growth.

3.3. Aerosol particle hygroscopicity

The hygroscopicity parameter κ is a measure of the affinity of the aerosol particles to water. Relatively high κ values greater than unitiy correspond to the highly hygroscopic inorganic species (e.g. sodium chloride; Petters and Kreidenweis, 2007) while oxidized

Table 1
Number of new particle formation events recorded each month for the years 2010 and 2011.

Month	NPF events (2010)	NPF events (2011)
January	0	–
February	0	2
March	2	5
April	5	8
May	9	10
June	13	11
July	6	3
August	2	7
September	2	7
October	3	4
November	2	1
December	2	0

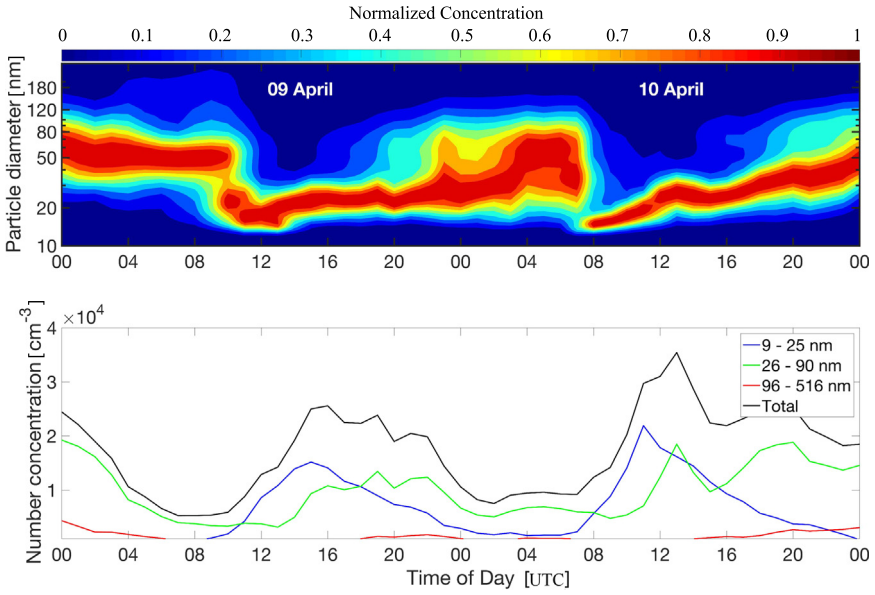

Fig. 9. Evolution of the particle size distributions during two consecutive NPF event days (9 and 10 April 2011). The upper panel shows hourly measurements of the aerosol size distribution (normalized by the maximum value), whereas the lower panel shows the number concentrations of the particles for four size ranges: 9–25 nm, 26–90 nm, 96–516 nm and 9–516 nm (total).

organic compounds found in the atmosphere have κ values in the range 0.01–0.3. In the case of multicomponent aerosol particles, κ can be estimated assuming that the total volume of water is equal to the sum of the water associated to the individual components (Petters and Kreidenweis, 2007) and can be calculated as $\kappa_{mixed} = \sum_i \varepsilon_i \kappa_i$, where ε_i is the volume fraction of each component having hygroscopic parameter κ_i.

Fig. 10 shows the diurnal pattern of the seasonally averaged κ distributions for particles having dry sizes of 165 and 35 nm. For all the particle sizes κ was below 0.5, suggesting the co-existence of organic and inorganic compounds in the aerosol phase during all seasons. The larger particles (i.e., those having dry diameters of 165 nm) show a constant diurnal pattern in all seasons. In winter and autumn the 165-nm particles exhibit an external mixing state with two distinct modes (85% of the days; cf. Fig. S7 for examples of daily measurement): one corresponding to the background aerosol with $\kappa \approx 0.4$ and a very hydrophobic mode with κ less than 0.1. The presence of this less hydroscopic mode becomes more dominant during periods with intense anthropogenic activities (i.e., traffic in the morning,

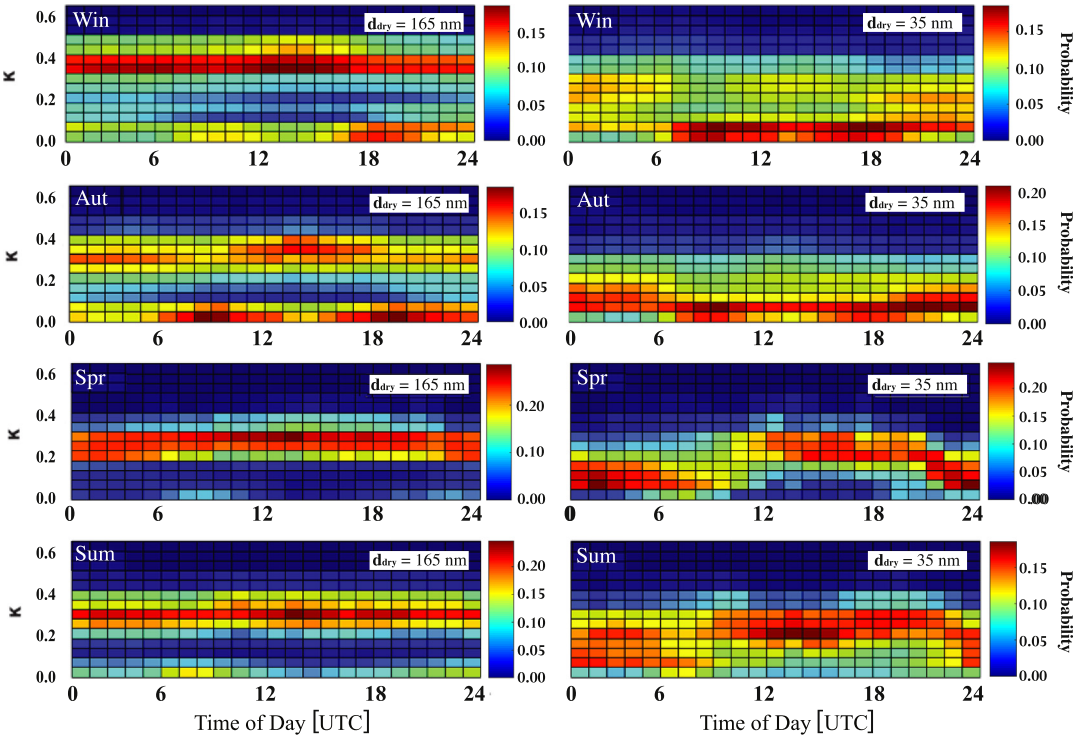

Fig. 10. Diurnal variation of the κ probability distributions of particles having dry diameters of 165 nm (left) and 35 nm (right).

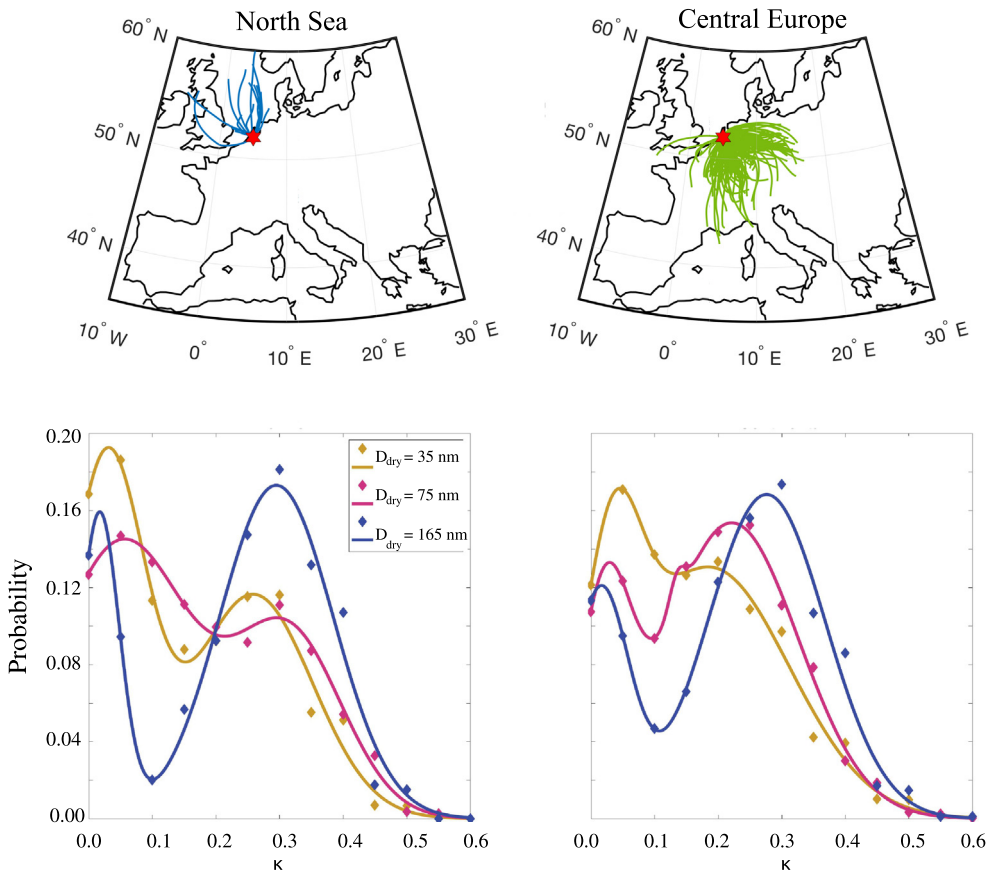

Fig. 11. Probability distributions of κ for different dry particle sizes carried to the station in marine (left) and continental (right) air masses.

between 06:00 and 12:00 UTC, and in the late evening, between 17:00 and 22:00 UTC, together with residential heating). In spring and summer, when the contribution of heating is minimum, the fraction of the less hygroscopic particles decreases markedly, resulting in an internally mixed aerosol with a mean κ of ca. 0.3 throughout the day, suggesting a strong influence from organic compounds.

The smaller particles (i.e., those having dry diameters of 35 nm) exhibit different diurnal patterns each season compared to the larger particles. In winter and autumn, when particles are emitted from anthropogenic sources between 07:00 and 19:00 UTC, their κ values are below 0.1. At night the distributions widen and the mean κ value is ca. 0.2. In spring and summer the distribution follows a different pattern: κ is 0.3 between 11:00 and 21:00 UTC but decreases to 0.15 during the night. The time of the shift to higher κ values coincides with the initiation of the NPF events. At night, when these processes ceise, κ shifts back to background values (i.e., around 0.1). The day-by-day analysis of the diurnal κ distributions showed that the seasonally averaged patterns (cf. Fig. 10) are representative for more than 85% of the days for winter, spring and summer. However, in autumn, some days exhibit a different pattern (e.g. narrower κ distributions) and the percentage of the days that resemble the seasonally averaged patterns drops to 60%.

Fig. 11 shows the κ probability distribution functions corresponding to air masses originating either from the North Sea (marine origin) or from Central Europe (continental origin). In all cases, the distributions are bimodal, with the smaller dry particles (35 nm in diameter) having a more pronounced hydrophobic mode and the larger particles (75 and 165 nm) a more pronounced hydrophilic mode. This similarity in the κ values when air masses from marine or continental origins reach the station indicates that particle hygroscopicity is mainly influenced by local sources.

4. Conclusions

In this study we report on a 8-year-long dataset (2008–2015) of aerosol particle mass concentrations ($PM_{2.5}$) and size distributions, as well as on a 10-month record of aerosol hygroscopicity at the CESAR site in The Netherlands. The yearly mean $PM_{2.5}$ concentrations showed a decreasing trend that can be attributed to more stringent regulations of industrial emissions and to the advanced emission treatment technologies introduced in the transportation sector over the past decade. $PM_{2.5}$ concentrations exhibit a clear seasonal variability which is primarily affected by the higher emissions and to a lesser extent by meteorological conditions such as the BLH and precipitation.

In contrast to the $PM_{2.5}$mass concentrations, the number concentrations of particles having diameters in the range 30–500 nm showed an increasing trend between 2008 and 2011 and an opposite trend from 2013 to 2015, with $N_{30\text{-}500}$ values in 2015 being at the same level with those in 2008, raising a concern on whether air quality actually improves as the $PM_{2.5}$ measurements suggest. Seasonally, $N_{30\text{-}500}$ was higher in spring and summer mostly due to the production of new particles by nucleation. The diurnal variation of the number concentration in winter and autumn shows pronounced peaks in the late morning and evening hours corresponding to traffic and residential heating patterns. The measurements also show a shift towards smaller particle sizes in spring and summer, supporting that the particle number concentrations during these seasons are strongly influenced by the nucleation events.

The hygroscopic parameter κ, of the particles of all the sizes measured in this work suggest the presence of organics in the particle phase. The freshly emitted smaller particles (35 nm) are most often

externally mixed compared to their chemically-aged larger counterparts (165 nm). The diurnal patterns of the seasonally averaged κ distributions of the larger particles were constant throughout the day while the smaller particles exhibited diurnal variations. The 165-nm particles are mostly internally mixed in spring and summer, whereas in autumn and winter the κ distributions are bimodal with the more hydrophobic peak being temporarily associated to traffic and residential heating. The smaller particles are externally mixed during all seasons and are also influenced by anthropogenic activities in the cold season as suggested be the reduced κ values during the day. In spring and summer, new particle formation events and photochemical aging are affecting the κ distributions, which are shifted to higher values during the day. Air masses of different origin (continental and marine) exhibit similar κ distributions for all sizes, highlighting the dominance of the local sources to particles hygroscopicity.

Data availability

1. Meteorological data can be obtained from the CESAR database http://www.cesar-_database.nl.
2. The SMPS data for the Cabauw station (Zijdeweg) are available at http://www.ebas.nilu.no.
3. The $PM_{2.5}$ for the Cabauw station (Wielsekade) data were provided from the National Institute for Public Health and the Environment (RIVM; contact person Rob Zwartjes, Rob.Zwartjes@rivm.nl).
4. The CAPE maps were obtained from http://www1.wetter3.de.

Competing interests

The authors declare that they have no competing interests.

Acknowledgments

We extend special appreciation to Mr. Rob Zwartjes of Rijksinstituut voor Volksgezondheid en Milieu (RIVM) for providing useful information about the PM measurements, to Mrs. Ann-Mari Fjæraa of the Norwegian Institute for Air Research (NILU) for providing level 0 SMPS data for quality check, as well as to Dr. Ari Asmi and Prof. Dr. Alfred Wiedensohler for providing valuable information regarding the SMPS measurements.

Appendix A. Supplementary data

Supplementary data to this article can be found online at https://doi.org/10.1016/j.scitotenv.2017.12.136.

References

CEN, 2005. 14907 Ambient Air Quality; Standard Gravimetric Measurement Method for the Determination of the $PM_{2.5}$ mass fraction of suspended particulate matter.

Asgharian, B., Price, O., Oldham, M., Chen, L.-C., Saunders, E., Gordon, T., Mikheev, V., Minard, K., Teeguarden, J., 2014. Computational modeling of nanoscale and microscale particle deposition, retention and dosimetry in the mouse respiratory tract. Inhal. Toxicol. 26, 829–842.

Baccarelli, A.A., Hales, N., Burnett, R.T., Jerrett, M., Mix, C., Dockery, D.W., Pope III, C.A., 2016. Particulate air pollution, exceptional aging, and rates of centenarians: a nationwide analysis of the United States, 1980–2010. Environ. Health Perspect. 124, 1744.

Birmili, W., Wiedensohler, A., Heintzenberg, J., Lehmann, K., 2001. Atmospheric particle number size distribution in Central Europe - statistical relations to air masses and meteorology. J. Geophys. Res. D: Atmos. 106, 32.

Boulon, J., Sellegri, K., Venzac, H., Picard, D., Weingartner, E., Wehrle, G., Collaud Coen, M., Bütikofer, R., Flückiger, E., Baltensperger, U., et al. 2010. New particle formation and ultrafine charged aerosol climatology at a high altitude site in the alps (Jungfraujoch, 3580 m asl, Switzerland). Atmos. Chem. Phys. 10, 9333–9349.

Bougiatioti, A., Bezantakos, S., Stavroulas, I., Kalivitis, N., Kokkalis, P., Biskos, G., Mihalopoulos, N., Papayannis, A., Nenes, A., 2016a. Biomass-burning impact on CCN number, hygroscopicity and cloud formation during summertime in the eastern Mediterranean. Atmos. Chem. Phys. 16, 7389–7409.

Bougiatioti, A., Nikolaou, P., Stavroulas, I., Kouvarakis, G., Weber, R., Nenes, A., Kanakidou, M., Mihalopoulos, N., 2016b. Particle water and pH in the eastern Mediterranean: source variability and implications for nutrient availability. Atmos. Chem. Phys. 16 (7), 4579–4591.

Dal Maso, M., Kulmala, M., Riipinen, I., Wagner, R., Hussein, T., Aalto, P.P., Lehtinen, K.E., 2005. Formation and growth of fresh atmospheric aerosols: eight years of aerosol size distribution data from SMEAR II, Hyytiala, Finland. Boreal Environ. Res. 10, 323.

Directive, 2008. 2008/1/EC of the European Parliament and of the Council of 21 December 2007 on Industrial Emissions (integrated pollution prevention and control).

Draxler, R.R., Hess, G., 1998. An overview of the HYSPLIT_4 modelling system for trajectories. Aust. Meteorol. Mag. 47, 295–308.

Draxler, R.R., Rolph, G., 2003. HYSPLIT (HYbrid Single-Particle Lagrangian Integrated Trajectory) model access via NOAA ARL READY website (http://www.arl.noaa.gov/ready/hysplit4.html). NOAA Air Resources Laboratory, Silver Spring.

Duplissy, J., Gysel, M., Sjogren, S., Meyer, N., Good, N., Kammermann, L., Michaud, V., Weigel, R., dos Santos, S.M., Gruening, C., et al. 2009. Intercomparison study of six HTDMAs: results and recommendations. Atmos. Meas. Tech.

EMEP EMEP/CEIP 2014 present state of emission data. http://www.ceip.at/webdab_emepdatabase/reported_emissiondata/.

EN 12341, 1998. C. A.: determination of the PM_{10} fraction of suspended particulate matter-reference method and field test procedure to demonstrate reference equivalence of measurement methods. European Committee for Standardization (European Standard EN 12341), Brussels.

Gallego, F.J., 2010. A population density grid of the European Union. Popul. Environ. 31, 460–473.

Gilbert, R.O., 1987. Statistical Methods for Environmental Pollution Monitoring. John Wiley & Sons.

Henzing, J., 2011. Interactive comment on: "number size distributions and seasonality of submicron particles in Europe 2008–2009" by A. Asmi et al.. Atmos. Chem. Phys. Discuss 11, C3137–C3142.

Jokinen, V., Mäkelä, J.M., 1997. Closed-loop arrangement with critical orifice for DMA sheath/excess flow system. J. Aerosol Sci. 28, 643–648.

Lelieveld, J., Evans, J., Fnais, M., Giannadaki, D., Pozzer, A., 2015. The contribution of outdoor air pollution sources to premature mortality on a global scale. Nature 525, 367–371.

Lohmann, U., Feichter, J., 2005. Global indirect aerosol effects: a review. Atmos. Chem. Phys. 5, 715–737.

Manders-Groot, A., Segers, A., Jonkers, S., Schaap, M., Timmermans, R., Hendriks, C., Sauter, R., Kruit, Wichink, van der Swaluw, E., Eskes, H., et al. 2016. LOTOS-EUROS v2. 0 reference guide.

Manninen, H., Nieminen, T., Asmi, E., Gagné, S., Häkkinen, S., Lehtipalo, K., Aalto, P., Vana, M., Mirme, A., Mirme, S., et al. 2010. EUCAARI ion spectrometer measurements at 12 European sites-analysis of new particle formation events. Atmos. Chem. Phys. 10, 7907–7927.

Matthijsen, J., Brink, H.M., Abels, M., Frink, C., 2007. $PM_{2.5}$ in The Netherlands: Consequences of the New European Air Quality Standards. Netherlands Environmental Assessment Agency.

Pal, S., Xueref-Remy, I., Ammoura, L., Chazette, P., Gibert, F., Royer, P., Dieudonné, E., Dupont, J.-C., Haeffelin, M., Lac, C., Lopez, M., Morille, Y., Ravetta, F., 2012. Spatio-temporal variability of the atmospheric boundary layer depth over the Parisag-glomeration: An assessment of the impact of the urban heat island intensity. Atmospheric Environ. 63, 261–275. https://doi.org/10.1016/j.atmosenv.2012.09.046. http://www.sciencedirect.com/science/article/pii/S135223101200917X.

Pal, S., Lee, T., Phelps, S., Wekker, S.D., 2014. Impact of atmospheric boundary layer depth variability and wind reversalon the diurnal variability of aerosol concentration at a valley site. Sci Total Environ 496, 424–434. https://doi.org/10.1016/j.scitotenv.2014.07.067. http://www.sciencedirect.com/science/article/pii/S0048969714010973.

Petters, M., Kreidenweis, S., 2007. A single parameter representation of hygroscopic growth and cloud condensation nucleus activity. Atmos. Chem. Phys. 7, 1961–1971.

Pope, I.C.A., Dockery, D.W., 2006. Health effects of fine particulate air pollution: lines that connect. J. Air Waste Manage. Assoc. 56, 709–742.

Ramanathan, V., Crutzen, P., Kiehl, J., Rosenfeld, D., 2001. Aerosols, climate, and the hydrological cycle. science 294, 2119–2124.

Russchenberg, H., Bosveld, F., Swart, D., ten Brink, H., de Leeuw, G., Uijlenhoet, R., Arbesser-Rastburg, B., van der Marel, H., Ligthart, L., Boers, R., et al. 2005. Ground-based atmospheric remote sensing in the netherlands: European outlook. IEICE Trans. Commun. 88, 2252–2258.

Seinfeld, J.H., Pandis, S.N., 2016. Atmospheric chemistry and physics: from air pollution to climate change. John Wiley & Sons.

Siakavaras, D., Samara, C., Petrakakis, M., Biskos, G., 2016. Nucleation events at a coastal city during the warm period: Kerbside versus urban background measurements. Atmos. Environ. 140, 60–68.

Solomon, S., 2007. Climate change 2007-The Physical Science Basis: Working Group I Contribution to the Fourth Assessment Report of the IPCC. vol. 4. Cambridge University Press.

Stolzenburg, M.R., McMurry, P.H., 1991. An ultrafine aerosol condensation nucleus counter. Aerosol Sci. Technol. 14, 48–65.

Triantafyllou, E., Diapouli, E., Tsilibari, E., Adamopoulos, A., Biskos, G., Eleftheriadis, K., 2016. Assessment of factors influencing PM mass concentration measured by gravimetric & beta attenuation techniques at a suburban site. Atmos. Environ. 131, 409–417.

US-EPA, 2004. Air Quality Criteria for Particulate Matter.

Wichmann, H.-E., Peters, A., 2000. Epidemiological evidence of the effects of ultra-fine particle exposure. Philos. Trans. R. Soc. Lond. A Math. Phys. Eng. Sci. 358, 2751–2769.

Wiedensohler, A., Birmili, W., Nowak, A., Sonntag, A., Weinhold, K., Merkel, M., Wehner, B., Tuch, T., Pfeifer, S., Fiebig, M., et al. 2012. Mobility particle size spectrometers: harmonization of technical standards and data structure to facilitate high quality long-term observations of atmospheric particle number size distributions. Atmos. Meas. Tech. 5, 657–685.

Winklmayr, W., Reischl, G., Lindner, A., Berner, A., 1991. A new electromobility spectrometer for the measurement of aerosol size distributions in the size range from 1 to 1000 nm. J. Aerosol Sci. 22, 289–296.

Zieger, P., Weingartner, E., Henzing, J., Moerman, M., Leeuw, G. d., Mikkilä, J., Ehn, M., Petäjä, T., Clémer, K., Roozendael, M. v., et al. 2011. Comparison of ambient aerosol extinction coefficients obtained from in-situ, MAX-DOAS and LIDAR measurements at Cabauw. Atmos. Chem. Phys. 11, 2603–2624.

Zlotkowska, R., 2015. Adverse health effects of the exposure to the spherical aerosol particles, including ultra-fine particles. Synergic Influence of Gaseous, Particulate, and Biological Pollutants on Human Health, pp. 109.